70(8A): 1-479; 2022. DOI: 10.18311/jmmf/2022/32015

Print ISSN : 0022-2755

Journal of Mines, Metals and Fuels

Contents available at: www.informaticsjournals.com/index.php/jmmf

Microstructure, Physical and Tensile Behaviour of B_4C Particles Reinforced Al7010 Alloy Composites

Kotresha Mydur[1*], Mahendra Kumar S[1], Madeva Nagaral[2], Bharath V[3], V Auradi[4]

[1]*Department of Mechanical Engineering, RV College of Engineering, Bangalore-560074, Visvesvaraya Technological University, Karnataka, India. Email: kotresha_mydur@rediffmail.com*
[2]*Aircraft Research and Design Centre, Hindustan Aeronautics Limited, Bangalore 560037, Karnataka, India*
[3]*Department of Mechanical Engineering, RNS Institute of Technology, Bangalore-560098, Visvesvaraya Technological University, Karnataka, India*
[4]*Department of Mechanical Engineering, Siddaganaga Institute of Technology, Tumakuru- 572103, Visvesvaraya Technological University, Karnataka, India*

Abstract

In the current studies an investigations were made to know the effect of 20 to 25 micron sized B_4C particles addition on the physical and mechanical behaviour of Al7010 alloy metal composites. Al7010 alloy with 4 and 8 wt.% of B_4C composites were produced by stir cast process. These synthesized composites were tested for numerous mechanical properties like hardness and tensile behaviour along with density measurements. Further, microstructural characterization was carried by SEM and XRD analysis to know the micron sized particles distribution and phases. By adding 20 to 25 micron sized B_4C particles hardness and tensile strength of Al7010 alloy was enriched with slight decrease in elongation. Further, density of Al7010 alloy was decreased with the accumulation of B_4C particles. Various tensile fracture behaviours were observed by SEM analysis.

Keywords: *Al7010 Alloy, B4C, Microstructure, Hardness, Tensile Behaviour, Fractography*

1.0 Introduction

With their exceptional quality and wear and fatigue resistance compared to traditional unreinforced materials, metal composites based on aluminium alloys have the potential to revolutionise aviation and defence applications [1]. Due to the movement of the load between the lattice and fortifications, Al-based MMCs require an enriched interfacial bond among Al grid and fortifications, which dictates the mechanical properties of the composites [2, 3].

Support material inserted into the metal increases the specific strength, stiffness, creep, and fatigue compared to standard engineering materials. Particle MMCs (fortified), short fibre supported (fortified), and continuous fibre strengthened and layered MMCs (fortified) can all be classified according to the support materials they are made from [4]. Preliminary studies have shown that the use of consistent fiber-enhanced MMC has been stymied by the high assembling costs of the fortification strands and the arduous assembly processes. As a result, their use has been restricted to the military and other extremely specialised fields. There has been a delay in the commercialization of fiber-strengthened MMCs despite the fact that these fortified MMCs have been shown to have superior

*Corresponding Author

thermal stability compared to particulate fortified materials [5, 6]. Because of their easy formability and low cost, particulate MMCs have recently been used in a variety of construction applications. Indeed, PAMCs have proven to be an excellent choice for a wide range of automotive and aerospace applications. These include braking mechanisms for trains as well as automobiles; gas turbine motors; helicopter engines; military aircraft and so on [7].

Wear resistance, stiffness, and indicated strength are all achieved by combining various types of particulate fortifications such as Al_2O_3, B_4C, Fly ash, ZrO_2, and so on with aluminium [8, 9]. With high modulus and resistance to thermal stress, these ceramic particles are widely used as a support in a variety of development materials. Improved rigidity of the composites was achieved by increasing the amount of aluminium amalgam particles in the mixture. B_4C improves the hardness and wear resistance of aluminum-boron carbide metal grid composites by acting as a lubricating film on the interaction surface and with low warm extension. B_4C improves the mechanical, wear resistance, and hardness of the material at high temperatures. Aluminum metal composites are primarily used in aircraft and vehicles because of their high explicit quality and strength as well as their excellent resistance to wear and tear.

This is because the mechanical requirements and desired properties of aluminium composites are closely tied to the preparation technique, and thus, the choice of creation process is critical [10, 11]. Delivery of aluminium composites is hindered by higher support material costs, non-homogeneous fortification dispersion in the framework, and sometimes higher venture costs. Composites' expanding range of uses depends on a well-thought-out assembly technique [12]. Stir casting, compo casting, infiltration, and powder metallurgy are the primary manufacturing techniques for mass metal composites [13].

A two-stage reinforcement addition method was used to make Al7010 composites by adding 4 and 8 wt.% of 20 to 25 micron sized B_4C particles. A further study was done on the mechanical properties of B_4C composites made of Al7010 alloy.

2.0 Experimental Details

Stir casting was used to create metal composites containing 4 and 8 weight per cent of B_4C particulates with a diameter of 20 to 25 microns. Al7010 was used as the main material, while B_4C particles with a diameter of 20 to 25 microns were taken as reinforcements, as shown in the Fig.1. Table 1 lists the alloy's chemical composition for the current investigation.

The liquid technique on stir casting technique is used to manufacture Al7010 alloy with 20 to 25 micron-sized reinforced B_4C composites. The electric furnace is loaded with Al7010 alloy metal blocks of a predetermined weight and heated to molten metal. The melting point of aluminium alloy is 660°C, but the metal is heated to a superheated 750°C. Thermocouples with the appropriate temperature range are used to measure melting and superheated temperatures, and these values are recorded. About three minutes of degassing with solid hexachloroethane (C_2C_{16}) is required to remove the gas from the crucible's superheated molten metal. The molten metal is stirred using a bladed fan type steel rotor coated with zirconia

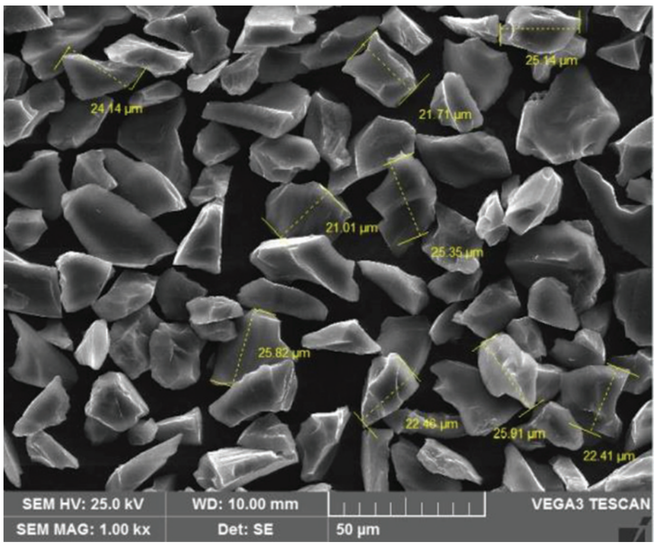

Figure 1: SEM micrograph of 20 to 25 micron sized B_4C particles

Table 1: Chemistry of Al7010 alloy by weight %								
Zn	Mg	Si	Fe	Cu	Ni	Mn	Cr	Al
6.70	2.60	0.12	0.15	2.0	0.05	0.10	0.05	Balance

Figure 2: Prepared Al7010 alloy B_4C composite

ceramic material. About 65% of the crucible is filled with molten metal, and the stirrer is submerged in the molten metal and rotated at approximately 300 rpm to create vortices in the metal. The pre-heated B_4C particles added into the Al molten material. Stirring continues until the Al7010 alloy matrix and B_4C reinforce particulates are completely wettable, at which point the interfacial shear strength is established as a result. To make the Al7010 alloy with a 4 per cent composite content, the molten metal of Al7010 matrix and B_4C is poured into cast iron moulds with dimensions of 120 mm in length and with a diameter of 15 mm. When producing composites with B_4C particulates, the same method is used, regardless of the percentage of composites. Fig.2 shows the composites of Al7010 alloy and B_4C that were prepared.

Scanning electronic microscopes are used to examine the microstructure of the Al7010 alloy, determining the even distribution of reinforcement particles. Al7010 alloy and Al7010 alloy with varying wt.% of B_4C reinforced composites microstructure images are taken. Microstructure specimens have a 15 mm dia., and a 5 mm height.

The densities of the Al7010 alloy with B_4C composites were analysed. According to the rule of mixture, the theoretical values were calculated, and the experimental densities used the standard weight method.

The hardness test specimen is machined in accordance with ASTM standard E10[14]. A Brinell hardness tester machine is used to measure the hardness. There is no roughness to the specimen's surface. The specimen has been subjected to a 250 kg load and a 5 mm ball indentation has been taken. The average of five indentation marks is taken into consideration.

Machined as per ASTM E8 standard [15] to study the tensile features of as-cast Al7010 alloy with varying wt.% B_4C particulate reinforced composites. It is used to measure the tensile strength of Al7010 alloy and B_4C composites under unidirectional tension, as well as to examine the effect of even dissemination on its behaviour. The specimen has an overall length of 104 millimetres, a gauge length of 45 millimetres, and a gauge diameter of 9 millimetres. The ultimate, yield, and elongation of a material can be determined by conducting this tensile test.

3.0 Results and Discussion

3.1 Microstructural Analysis

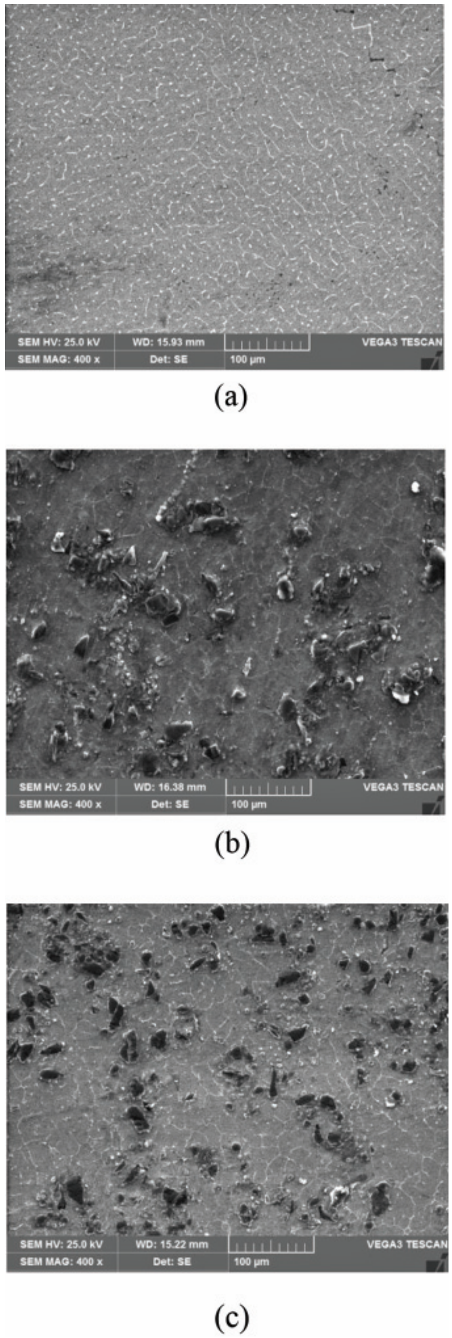

Figure 3: SEM of (a) Al7010 alloy (b) Al7010 with 4 wt. % B4C (c) Al7010 with 8 wt. % B_4C composites

Microphotographs of the SEM images of Al7010 alloy, Al7010 with 4 and 8 wt.% B4C composites are shown in Fig.3(a-c). The SEM image of Al7010 alloy can be seen in Fig.3(a). This shows the distinct grain boundaries without the presence of any particles. There are no voids or other casting flaws visible on the micrograph. Fig.3 (b-c) shows micrographs of Al7010-4 wt.% of B_4C, and Al7010-8 wt.% of B_4C composites. For B_4C reinforced composites, micro-particles can be clearly seen in the images taken with a microscope. By employing a novel, two-step stir casting route, these composites are free from clustering and agglomeration. Furthermore, the microstructure surface of Al7010 alloy with 8 wt.% B_4C composites microstructure contains many particles and also these are distributed throughout the matrix Al7010 matrix.

A typical XRD pattern of Al7010 alloy is shown in Fig.4a, where various aluminium phases can be seen at various peaks. At 39, 45, 65, and 79, the presence of Al phases is confirmed with varying intensities. At a wavelength of 39, the Al phase reaches its peak intensity. Al7010 alloy with 8% B_4C particulates reinforced composites is depicted in Fig.4(b). Phases like Al and B_4C are shown in Fig.4(b). As previously stated, there are numerous Al and B_4C particles phases available at various 2 angles with varying intensities, as shown in the figure.

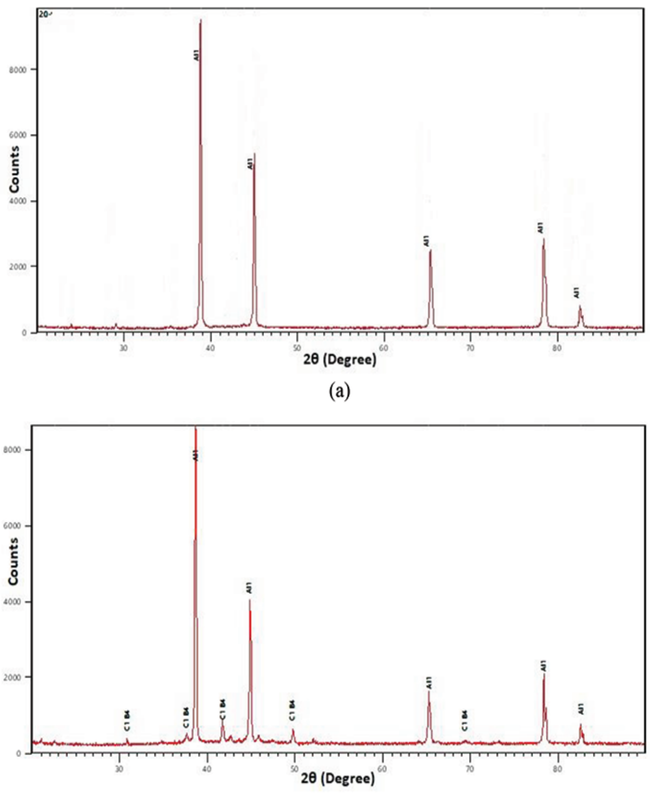

Figure 4: X-ray diffraction patterns of (a) Al7010 alloy (b) Al7010-8 wt. % B_4C composites

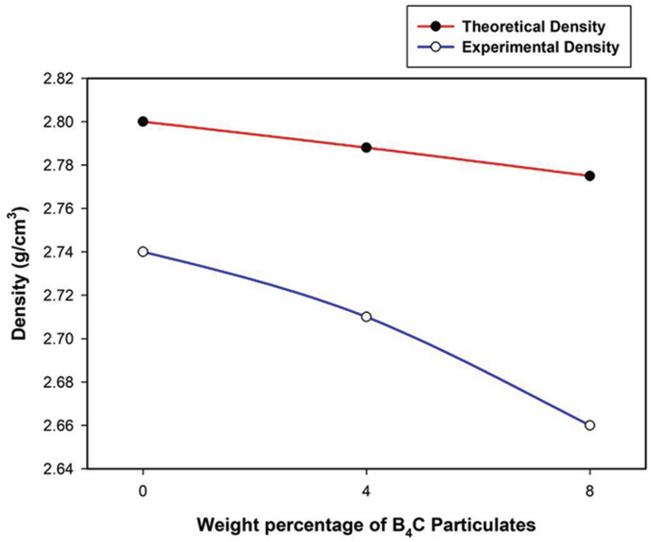

Figure 5: Densities of Al7010 alloy with B_4C composites

3.2 Density Measurements

Fig.5 shows the density differences between the Al7010 and Al7010 with 4 and 8 wt.% B_4C reinforced composites. The rule of mixture is used to calculate the theoretical density of Al7010 alloy and B_4C composites. Furthermore, the weight concept is used to determine the experimental densities. In the study, B_4C particles had a density of 2.52 g/cc, which is lower than Al7010 alloy's theoretical density of 2.80. The density of the base alloy decreased from 2.80 g/cc to 2.775 g/cc as the wt.% of B_4C particles in the Al7010 matrix increased from 4 to 8 wt.%. Because B_4C particles have a lower density than Al matrix, their incorporation results in a decrease in density [16]. The overall density of the matrix is reduced as a result of the lower density of the reinforced particles. To make matters even more confusing, a quick glance at the graph shows that actual density values are only a tiny fraction of theoretical values.

3.3 Hardness Measurements

Fig.6 depicts the hardness of Al7010 and Al7010 with B_4C micro particles composites. The hardness of Al7010 alloy increases as the percentage of B_4C particles in the alloy increases from 4% to 8%, according to the plot. The hardness of Al7010 alloy is 65.5 BHN, in 4 wt.% of B_4C composites it is 81.3 BHN. Further, 8 wt.% of B_4C composites have 97.8 BHN. As the grain size of the filler is influenced by the presence of micro particles,

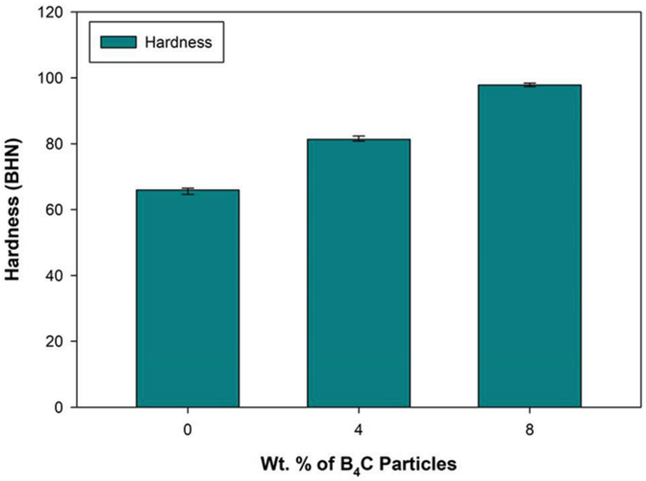

Figure 6: Hardness of Al7010 alloy with B4C composites

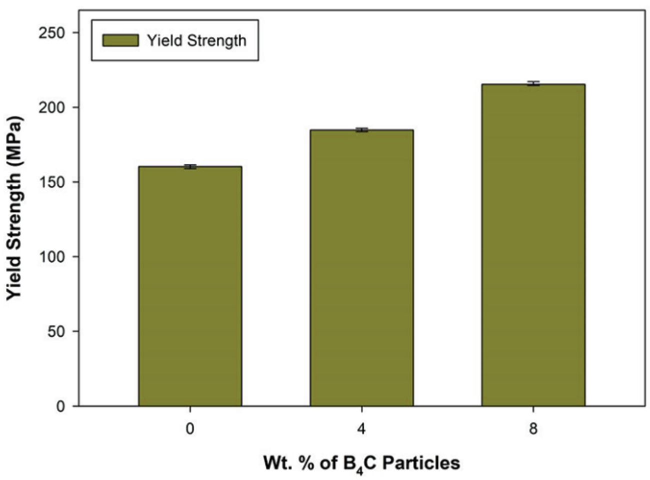

Figure 8: Yield strength of Al7010 with B_4C composites

an increase in hardness can be expected [17]. Adding micro particles to Al7010-B_4C composites can inhibit grain growth, progress crystal grains in the matrix, and have an impact on the refined composites.

3.4 Ultimate Tensile and Yield Strength

Figures 7 and 8 show the impact of B_4C particles with a diameter of 20 to 25 microns on the ultimate and yield strengths of an Al7010 alloy. Addition of B_4C has increased Al7010 alloy's tensile strength. This alloy has an ultimate and yield strength of 185.1MPa and 147.2MPa. Al7010 alloy with 8 wt.% B_4C particle composites has an ultimate and yield strength of 285.2 and 228.9 MPa, respectively. The strength of Al7010 has amplified more as the percentage of B_4C in the alloy increases from 4 to 8 wt. per cent.

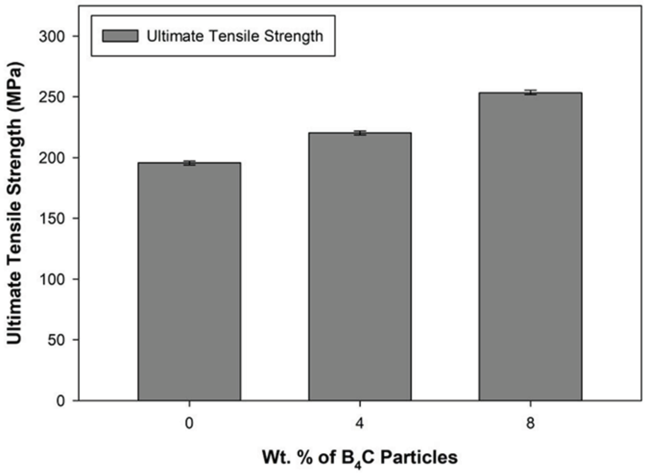

Figure 7: Ultimate strength of Al7010 with B_4C composites

The presence of micron-sized B_4C particles in the base Al7010 contributes to the alloy's increased strength. The thermal mismatch strain may follow up on the matrix as pre-stress, or it may discharge the disengagement loop and remove warm pressure. When the lattice material expands due to B_4C, it increases its dislocation density, which acts as a support effect on the Al network [18]. The Al7010 amalgam with B_4C composites is stronger as a result of the expansion in dislocation density. For composites made from aluminium alloys such as aluminium alloy Al7010, B_4C is a good choice because it acts as a barrier to particle dispersion and as a reinforcement of the matrix, preventing separation and improving the quality of the composites [19].

3.5. Percentage Elongation

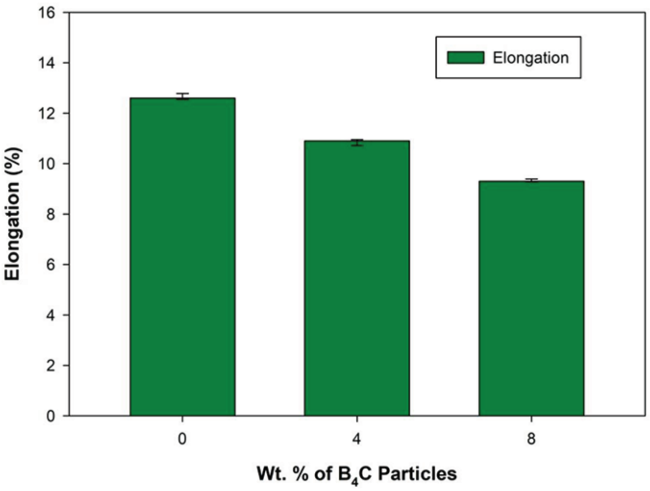

Figure 9: Percentage elongation of Al7010 with B_4C composites

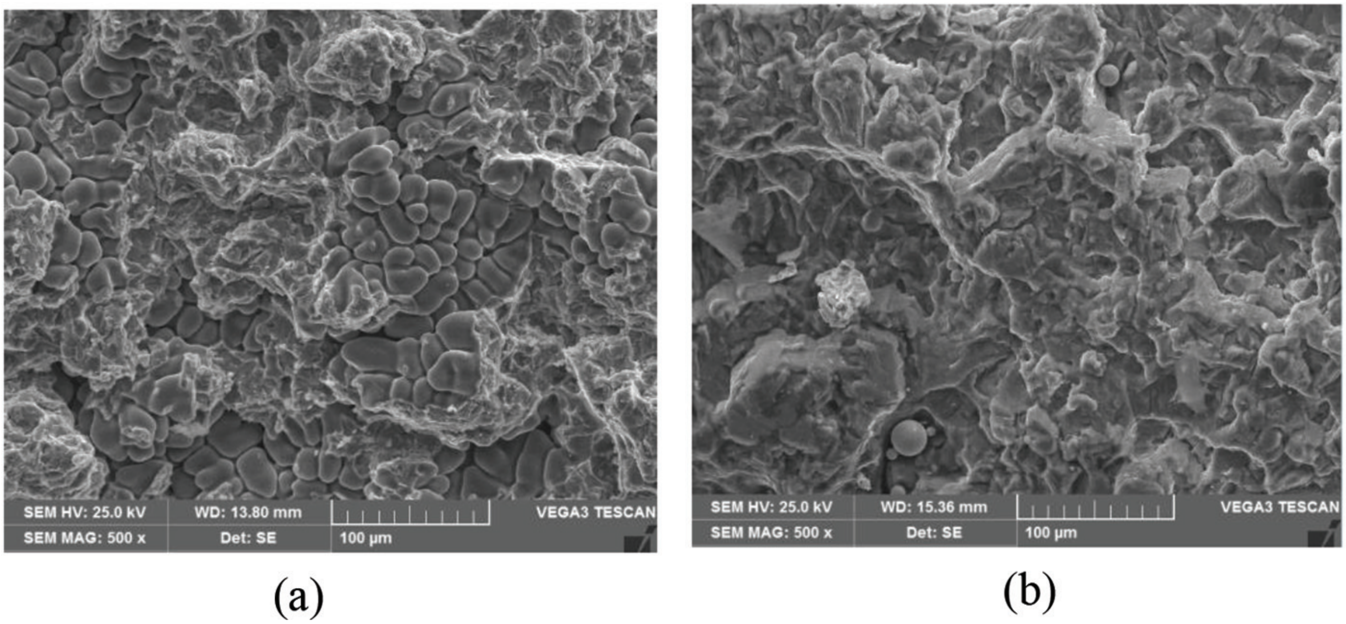

Figure 10: SEM images of tensile fractured surfaces of (a) Al7010 alloy (b) Al7010 with 8 wt.% of B_4C composites

Fig.9 depicts the effect of 20 to 25 micron-sized B_4C particles on the Al7010 alloy's ductility. Al7010's ductility diminished as a result of B_4C particles. The presence of hard B_4C particles is to blame for this reduced ductility. As the B_4C content rises to 8 wt.%, the ductility decreases even more. The deformation of the Al7010 alloy matrix is limited by the presence of these particles.

3.6 Tensile Fractography

Fig. 10 depicts the fractured surfaces of Al7010 alloy and boron carbide composites made from it. An example of plastic fracture morphology is shown in Fig.10(a). Al7010 fractures look like those shown in Fig.13(a). An Al7010 alloy with 8 wt.% B_4C micro composites is depicted in Fig.10 (b). Al/B4C composite dimple sizes and depths are altered when hard particles are added. Because of the brittle fracture morphology caused by boron carbide, this is a critical morphology indicator. Crack propagation along the interface of metal composites during the fracture process disperses a small quantity of particles at the edge of the dimple. Carbide particles in the Al7010 material cause the matrix to be more brittle when the mass fraction of carbide particles in the alloy increases.

4.0 Conclusions

Stir technique was used to make Al7010 reinforced composites with B_4C particles of 20 to 25 micron size, with B_4C particle weight percentages ranging from 4 to 8 wt.%. The microstructure with density-hardness and tensile characteristics of Al7010 alloy metal composites were studied. SEM microphotographs show that the composites are free of pores and have a uniform distribution of micro particles. The XRD analysis shows that the Al7010 alloy matrix contains boron carbide particles. The B_4C particles reinforced composites outperformed the Al7010 alloy in terms of hardness and tensile strength. When related to the Al7010 alloy, metal composites had a slightly lower density. Using a tensile fractured surface as a guide, one can determine the nature of the fracture.

References

[1] Pankaj R jadhav, B R Sridhar, Madeva Nagaral and Jayasheel I Harti, "Mechanical behaviour and fractography of graphite and boron carbide particulates reinforced A356 alloy hybrid metal matrix composites", *Advanced Composites and Hybrid Materials*, 3, 2020, pp. 114- 119.

[2] Prasad H Nayak, H K Srinivas, Madeva Nagaral, "Characterization of tensile fractography of nano ZrO_2 reinforced copper-zinc alloy composites", *Frattura ed Integrity Strutturale* (Fracture and Structural Integrity), 48, 2019, pp. 370-376.

[3] N. G. Siddesh Kumar, G. S. Shivashankar, S. Basavarajappa, R. Suresh, Some studies on

mechanical and machining characteristics of Al2219/n-B_4C/MoS2 nano hybrid metal matrix composites, *Measurement*, 107, 2017, pp. 1-11.

[4] C. S. Ramesh, R. Noor Ahmed, M. A. Mujeebu, M. Z. Abdullah, "Development and performance analysis of novel cast copper SiC-Gr hybrid composite", *Materials and Design*, 30, 2009, pp. 1957-1965.

[5] H S Kumar, U N Kempaiah, Madeva Nagaral, V Auradi, "Impact, Tensile and Fatigue Failure Analysis of Boron Carbide Particles Reinforced Al-Mg-Si (Al6061) Alloy Composites", *Journal of Failure Analysis and Prevention*, 21, 6, 2021, pp. 2177-2189.

[6] Reddy A. Chennakesava, "Tensile fracture behaviors of 7072/SiCp metal matrix composites fabricated by gravity die casting process", *Materials Technology,* 26, 5, 2011, 257.

[7] R M Wang, M K Surappa, C H Tao, C Z Li, M G Yan, "Microstructure and interface structure studies of SiC reinforced Al6061 metal matrix composites", *Materials Science and Engineering* A, 254, 1998, pp. 219-226.

[8] S A Sajjadi, M Torabi Parizi, H R Ezatpour, A Sedghi, Fabrication of A356 composite reinforced with micro and nano Al_2O_3 particles by a developed compo- casting method and study of its properties, *Journal of Alloys and Compounds*, 511, 2014, pp. 226-231.

[9] GL Chandrasekhar, Y Vijayakumar, Madeva Nagaral, C Anilkumar, "Microstructural Evaluation and Mechanical Behaviour of Nano B_4C Reinforced Al7475 Alloy Metal Composites", *International Journal of Vehicle Structures & Systems*, 13, 5, 2021, pp. 673-677.

[10] Dinesh Patidar, R S Rana, Effect of B4C reinforcement on the various properties of aluminium matrix composites: a survey paper, Materials Today Proceedings, 4, 2017, pp. 2981-2988.

[11] G B Veereshkumar, "Assessment of mechanical and tribological characteristics of Silicon Nitride reinforced aluminium metal matrix composites", Composites Part B: *Engineering,* 175, 2019, 107138.

[12] Jayasheel I Harti, B R Sridhar, H R Vitala, Pankaj R Jadhav, "Wear behaviour of Al2219-TiC particulate metal matrix composites", *American Journal of Materials Science*, 5, 3C, 2015, pp.34-37.

[13] S Matti, B P Shivakumar, S Shashidhar, M Nagaral, "Dry sliding wear behaviour of mica, fly ash and red mud particles reinforced Al7075 alloy hybrid metal matrix composites", *Indian Journal of Science and Technology*, 14, 4, 2021, pp. 310-318.

[14] T. Rajmohan, K. Palanikumar, S. Ranganathan, "Evaluation of mechanical and wear properties of hybrid aluminium matrix composites", *Transactions of Nonferrous Metals Society of China*, 23, 2013, pp. 2509-2517.

[15] K. Kalaiselvan, N. Murugan, Siva Parameshwaran, Production and characterization of AA6061-B_4C stir cast composite, *Materials and Design*, 32, 2011, pp. 4004-4009.

[16] T.H. Raju, R. S. Kumar, S. Udayashankar, A. Gajakos, Influence of Dual reinforcement on Mechanical Characteristics of Hot Rolled AA7075/Si_3N_4/Graphite MMCs, *Journal of The Institution of Engineers* (India): Series D, Volume 102, 2021.

[17] T. Hemanth Raju, B.B. Chandan , S. Belagavi Vinaya, T. J. Udayashankar, Amit Kumar Gajakosh, Influence of zircon particles on the characterization of Al7050-Zircon composites, Materials Today Proceedings, Volume 47, 2021.

[18] U. B. Krishna, B. Vasudeva, Virupaxi Auradi, Madeva Nagaral, Mechanical characterization and tensile fractography of Al7075-WCP-CoP composite, *Frattura e Integrita Strutturale*, 60, 2022.

[19] Zeeshan Ali, V Muthuraman, P Rathnakumar, P Gurusamy, Madeva Nagaral, Studies on mechanical properties of 3 wt.% of 40 and 90 μm size B_4C particulates reinforced A356 alloy composites, Materials Today: Proceedings, 52, 2022, pp. 494-499.